Journal of Cardiovascular Translational Research (2023) 16:127–140
https://doi.org/10.1007/s12265-022-10277-2

ORIGINAL ARTICLE

Periplocin Alleviates Cardiac Remodeling in DOCA-Salt–Induced Heart Failure Rats

Jiameng Hao[1,2] · Liping Chang[1,2] · Dandong Wang[1,2] · Chuanyuan Ji[2,3] · Shaolan Zhang[2,4] · Yunlong Hou[1,2] · Yiling Wu[1,2]

Received: 23 January 2022 / Accepted: 17 May 2022 / Published online: 26 May 2022

Abstract

Heart failure with preserved ejection fraction (HFpEF) is a common public health problem associated with increased morbidity and long-term mortality. However, effective treatment for HFpEF was not discovered yet. In the present study, we aimed to decipher the effects of Periplocin on DOCA-induced heart failure rats and explore the possible underlying mechanisms. We demonstrated that Periplocin could significantly attenuate cardiac structural remodeling and improve cardiac diastolic function. Of note, Periplocin significantly inhibited the recruitment of inflammatory and immune cells and decreased the expression of serum inflammatory cytokines. Meanwhile, Periplocin had the effect of cardiac glycosides to improve cardiomyocyte contractility and calcium transient amplitude. These findings indicate that Periplocin might be a potential medicine to treat HFpEF in patients.

Keywords HFpEF · Periplocin · Cardiac remodeling · Inflammation

Abbreviations

HFpEF	Heart failure with preserved ejection fraction
DOCA	Deoxycorticosterone acetate
H&E	Hematoxylin and eosin
WGA	Wheat germ agglutinin
NT-pro BNP	N-terminal B-type natriuretic peptide precursor
LVAW	Left ventricular anterior wall
LVPW	Left ventricular posterior wall
IVRT	Isovolumic relaxation time
LVCT	Isovolumic contraction time
E	Passive peak left ventricular filling velocity
A	Peak atrial systolic flow velocity
F.S.	Fractional shortening
E.F.	Ejection fraction
S.V.	Stroke volume
EDP	End-diastolic pressure
LVP	Left ventricular pressure
CVF	Collagen volume fraction
CSA	Cross-sectional area
EDPVR	End-diastolic pressure–volume relationship
ESPVR	End-systolic pressure–volume relationship
MMP9	Matrix metallopeptidase 9
NF-κB	Nuclear factor kappa-B
TGF-β	Transforming growth factor-β
GM-CSF	Granulocyte-macrophage colony-stimulating factor
IFN-γ	Interferon-γ
ICAM-1	Intercellular cell adhesion molecule-1
IL	Interleukin

Associate Editor Nicola Smart oversaw the review of this article

✉ Yunlong Hou
houyunlonghrb@hotmail.com

✉ Yiling Wu
professorylw@163.com

[1] Hebei Medical University, Shijiazhuang 050017, Hebei, China

[2] Key Laboratory Cardio-Cerebral Vessel Collateral Disease, State Administration of Traditional Chinese Medicine, Shijiazhuang 050023, Hebei, China

[3] Nanjing University of Traditional Chinese Medicine, Nanjing 210023, Jiangsu, China

[4] Hebei University of Traditional Chinese Medicine, Shijiazhuang 050091, Hebei, China

Introduction

Heart failure with preserved ejection fraction (HFpEF), characterized by an ejection fraction (EF) higher than 50% and changes in myocardial structure and cardiomyocyte function, including cardiomyocyte hypertrophy and fibrosis, is the most common form of heart failure which affects over 37 million worldwide and imposes an enormous burden on global healthcare [1, 2]. In China, the prevalence of HFpEF is 3.5%, which makes it a pressing clinical event associated with high mortality and hospitalization rates [3]. Currently, there are no reliable treatments that could improve the prognosis and reduce cardiovascular mortality in patients with HFpEF [4]. HFpEF is a heterogeneous cardiovascular syndrome that is often accompanied by pro-inflammatory and metabolic related co-morbidities [5]. Noncardiac co-morbidities, such as overweight/obesity, hypertension, diabetes, and chronic obstructive pulmonary disease, which release pro-inflammatory cytokines, have the potential to induce a systemic pro-inflammatory state [6]. A systemic pro-inflammatory state has been proved to be responsible for structural and functional changes in the myocardium [5], including abnormal diastolic relaxation, impaired left ventricle filling, increased myocardial stiffness, impaired vascular compliance, left ventricular remodeling, and hypertrophy [7]. Anti-inflammatory therapy may benefit a subset of HFpEF patients [8].

Cardiac glycoside can directly enhance myocardial contractility, especially in the failing heart [9]. By reason of the ventricular systolic function is usually normal or only mildly impaired in patients with HFpEF, the profit of cardiac glycoside may be limited. Nevertheless, it still has considerable benefit in improving energy-dependent diastolic early myocardial function [10] and regulating neurohormone levels [11]. Studies have shown that digitalis cardiac glycosides can significantly improve hemodynamics [12], reduce myocardial ischemia [13], decrease left ventricular end-diastolic volume [14], and increase right ventricular inotropic status [15] in patients with preserved left ventricular function. In terms of improving myocardial compliance, digitalis glycosides can reduce the degree of LV hypertrophy, reduce the collagen content, and increase the dP/dt min index [16]. When applicate in a short-term period, digitalis cardiac glycosides can also produce some benefits, including enhancing mitochondrial function, promoting rapid and complete ventricular diastole, increasing visceral blood flow, and increasing venous volume [17]. Although it is still contentious whether cardiac glycoside can be used in the treatment of HFpEF, increasing research attention investigated the novel therapeutic potential of cardiac glycosides in HFpEF treatment, which provides excellent examples to illustrate our strategy.

Cortex Periplocae (Xiangjiapi), which can relieve swelling, dispel rheumatism, and strengthen muscles and bones [18], is the dried root bark of *Periploca sepium Bge* (the family of Lauraceae). Periplocin, a class of alpha-pyrogenic glycosides present in Cortex Periplocae, exhibits various pharmacological effects, such as cardiotonic diuretic, antitumor, anti-inflammatory, and immunomodulatory [19–21]. Periplocin, the most substantial cardiotonic effect among the four cardiac glycosides in Xiangjiapi, can selectively act on the heart and strengthen positive inotropic force by increasing myocardial contractility and slowing down the heart rate [22]. Research reported that Periplocin could improve left ventricular systolic pressure (LVSP), left ventricular end-diastolic pressure (LVEDP), + dP /dt Max, and -dP/dt Max, and other cardiac function indices [23]. Ma L. et al. [24] found that Periplocin could improve the left ventricular structure and function, and increase the SERCA mRNA expression in rats with chronic heart failure (CHF).

Given its cardiotonic and anti-inflammatory effects, Periplocin may have therapeutic effect on HFpEF. Accordingly, this study aimed to explore the therapeutic effects of Periplocin, in rats with DOCA-induced hypertension heart failure, on cardiac function, cardiac structural remodeling, and the deleterious effects due to the increased systemic pro-inflammatory state.

Methods

Animal Model and Experimental Protocol

Male SD rats (180–200 g), obtained from Vital River Laboratory Animal Technology Co. Ltd (Beijing, China, license number SCXK2016-0006), were housed in a well-controlled environment with a 12-h light/dark cycle at room temperature (23 ± 2 °C). Foods and water were supplied continuously. Rats were randomly divided into three groups: normal group ($n = 15$), model group ($n = 15$), and Periplocin group (1.5 mg/kg, $n = 15$). Rats in the normal group were untreated. Rats in other groups were induced HFpEF as published [25]. Briefly, firstly, for mono-nephrectomy, the animals were anesthetized with pentobarbital sodium (25 mg/kg, i.p.) by intraperitoneal injection. Subsequently, the left renal vessels and ureter were ligated from a longitudinal incision made on the side of the abdomen. Afterwards, the incision site was sutured with a sterile suture needle. Postoperative rest and penicillin (100,000 units/day) injection were continued for 3 days. After mono-nephrectomy, rats were injected with DOCA (25 mg/kg, i.h., Aladdin Biochemical Technology Co. Ltd, China) and given 1% sodium chloride in drinking water for 4 weeks to induce induced HFpEF. Rats in Periplocin group were given Periplocin (1.5 mg/kg) by oral gavage daily for additional 8 weeks. Blood pressure

was measured every 2 weeks after treatment through the Tail-Cuff method (BP-2000; Visitech Systems, USA) until the end of 12 weeks. All animals were handled and maintained under the Animal Care and Use Committee of Hebei Yiling Chinese Medicine Research Institute (Shijiazhuang, China).

Biomarker's Assessments

The N-terminal B-type natriuretic peptide precursor (NT-proBNP) was obtained using Enzyme-Linked Immunosorbent Assay Kits (Immunoway, USA) to evaluate the cardiac function. At the end of the 12-week experiment, blood samples from the abdominal aorta were collected, gently inverted more than 10 times, and placed on ice before further centrifuge. Blood samples were centrifuged at 1800 g for 10 min and the upper serum samples obtained were centrifuged at 13000 g for 2 min again, and standby for the test.

Morphological Analysis and Immunofluorescence Staining

Hearts dissected from the executed animals were fixed in 10% formalin solution, dehydrated with ethanol, embedded into paraffin, and sectioned at 4 μm parallel to the apical-basal axis for hematoxylin/eosin (H&E) staining and Masson's trichrome staining (Life Sciences, China). The collagen volume fraction (CVF) was calculated as the total area of fibrosis (defined as the amount of collagen deposited by aniline blue staining) divided by the sum of the total tissue area of the five random fields on each section. Alexa Fluor 488-conjugated wheat germ agglutinin (Thermo Fisher Scientific, USA) and α-SMA (Abcam, U.K.) antibodies were used to assess the cross-sectional area (CSA) of cardiomyocytes. Five randomly selected segments of each group were evaluated in a blinded manner, and representative images were selected to show in the figures.

Echocardiographic Measurements

Rats were anesthetized in a 1% isoflurane oxygen mixture and then underwent echocardiography (Vevo 3100 LT, FUJIFILM VisualSonics, Canada). Standard 2D and M-mode images, obtained in parasternal long-axis views and mid wall transverse views of the left ventricle, were used to guide the calculation of heart rate, fractional shortening (F.S.), ejection fraction (E.F.), stroke volume (S.V.), left ventricular anterior/posterior wall thickness (LVAW/LVPW), isovolumic relaxation time (IVRT), isovolumic contraction time (LVCT), and left ventricular diameters. Passive peak left ventricular filling velocity E (cm/s) and peak atrial systolic flow velocity A (cm/s) were obtained from mitral Doppler flow images in four-chamber heart views. In echocardiographic studies, the rat's heart rate was maintained in the range of 250–350 beats per minute. Measurements of diastolic function, especially the relationship between early and late filling (E/A ratio), were reported.

Hemodynamic Measurements

Under general anesthesia, an invasive hemodynamic study was performed at the end of 12-week experiment to assess cardiac function. Left ventricular dP/dt Max/Min, LV pressure (LVP) at end-diastolic pressure (EDP), Diastolic Duration, Tau, end-diastolic pressure–volume relationship (EDPVR), and end-systolic pressure–volume relationship (ESPVR) were measured through the right carotid artery with 7-Fr combined catheter manometer (Millar instrument, Houston, USA). The data was recorded for 20 min until the hemodynamic parameters reached a steady-state, and the last ~ 100 cardiac cycles were used for calculations. All pressure–volume loop data were recorded at least 8 to 10 beats at end-expiration from the raw LV pressure, and using LabChart8 software (ADInstruments, Australia) obtained conductance volume data.

Western Blot Analysis

Protein samples were prepared from cardiomyocytes isolated from rat and protein concentration was estimated by the BCA method. Lysates containing 50 μg protein were separated by electrophoresis on a SDS PAGE gel and then transferred to a nitrocellulose membrane (Pall Corporation, California, USA) by wet transfer method. After blocking with 5% bovine serum albumin for 1 h, the membranes were probed with one of the following primary antibodies: anti-Matrix metallopeptidase 9 (MMP9, 1:10000, Abcam, USA), anti-nuclear factor kappa-B (NF-κB p65, 1:1000, Abcam, USA), anti-Transforming Growth Factor Beta 1 (TGF-β, 1:1000, Abcam, USA), and anti-GAPDH (loading control, 1:10000; Abcam, USA) overnight at 4 °C. After washing in Tris-buffered saline Tween (TBST), the nitrocellulose membrane was incubated with the secondary antibody of Goat Anti-Rabbit IgG H&L preabsorbed (1:10000, Abcam, USA) for 1 h at room temperature. Finally, the membranes were imaged with a Bio-Rad Calibrated Densitometer system, and intensity of immunoblot bands was normalized to that of the loading control (GAPDH).

Cell Shortening and Calcium Transient Measurements

Ventricular myocytes were isolated from the hearts of adult wild-type SD rats, and the isolated hearts were perfused with collagenase retrogradely by the Langendorff device. As described previously [26, 27], calcium-free solution was

used as perfusion solution. After digesting with collagenase II solution, the myocytes were collected into KB solution, gradient coated with calcium, and stored on ice. Myocytes were loaded with the calcium fluorescent probe Fura-2-AM (ab120873, Abcam, USA) into the cardiomyocytes for 10 min. The contraction of ventricular myocytes was evaluated using the IonOptix (Milton, USA) cardiomyocyte AM detection system, and the stimulation voltage is 10 V at the frequency in 1 Hz. The following parameters were recorded: cell shortening (bl/ph%), Fura-2 ratio (bl/ph%), 10% of the peak (Tp), and the time to 10% of the baseline (Tr). After measuring the basic contraction and calcium fluorescence intensity, Periplocin (0.1, 1, 3, 10, 30 μM) was added to observe its effect on myocardial cell contraction and calcium transient.

Inflammatory Cytokine Measurements (Luminex Assay)

Rat plasma inflammatory cytokine levels were measured by using Luminex MAGPIX Multiplex Immunoassay System according to the manufacturer's instructions. Fifteen cytokines, including C-X-C Motif Chemokine Ligand 3 (CXCL3), granulocyte–macrophage colony-stimulating factor (GM-CSF), Intercellular Adhesion Molecule 1 (ICAM-1), interferon-γ (IFN-γ), Interleukin (IL)-1α, IL-1β, IL-2, IL-4, IL-6, IL-10, IL-18, L-Selection, Tissue Inhibitor of Metalloproteinases 1 (TIMP-1), Tumor Necrosis Factor (TNF-α), vascular endothelial growth factor (VEGF), were measured. Briefly, diluted plasma was cultured with premixed magnetic particles at room temperature for 2 h. After washing, the plasma was incubated with the antibody mixture for 1 h. Next, plasma was incubated with streptavidin PE at 800 rpm for 30 min. At the end, add 100 μL of Wash Buffer to each well, incubate for 2 min at RT, then use a Luminex® analyzer read within 90 min.

Flow Cytometry

The splenocytes were extracted as published [28]. In brief, the spleen was ground in precooled PBS buffer and splenocytes were suspended in 5 mL RMPI 1640 medium. After centrifugation at 150 g, the cell pellet was resuspended in 0.4 mL of RBC lysis buffer (Beyotime Biotechnology, China) and lysed for 5 min at room temperature to remove the red blood cells. Repeat with the centrifugation and resuspended the splenocytes pellet in fresh RMPI 1640. Blood PBMC were isolated with the following protocol: heparin anticoagulant peripheral blood was collected, added on to appropriate separation solution, and centrifuged at 800 g for 25 min. The PBMC interface was carefully removed by aspirating between the separation solution layer and the plasma layer. Washed with PBS for 3 times by centrifugation at 250 g for 10 min, then resuspended in 400μL RMPI 1640 medium and set aside for further use, taking 400μL of 1×10^7 cells for flow cytometry backup.

Isolated single-cell suspensions were incubated in a fluorophore-labeled monoclonal antibody cocktail for 50 min at room temperature. Antibody selection and activated macrophages/monocytes were identified with different antibody panels: Lineage 1: CD3-FITC, CD4-Perp Cy5.5, CD8-PE Cy7, IFN-γ-AF647, IL-4-PE (BioLegend, USA) for detection of T-lymphocytes and their Th1 and Th2 subtypes; Lineage 2: CD3-FITC, CD4-Perp Cy5.5, CD25-PE, Foxp3-AF647 (BioLegend, USA) for Treg subtype detection; Lineage 3: CD45-FITC, CD11b/c-PE (BioLegend, USA) for macrophage/monocyte subpopulation identification.

Statistics

All data are expressed as standard error (Mean ± SEM). If variances were homogeneous, the statistics were carried out by one-way analysis of variables (ANOVA) and the least significant difference (LSD) test was used for comparison between groups. The post hoc test of uneven variance adopts Dunnett's T3. Set the p-value to < 0.05 as statistically significant. Statistics were performed with SPSS 22.0 software (IBM, USA).

Results

Periplocin Protected the Heart Against Hypertensive Cardiac Remodeling in Rats with HFpEF

The experiment was designed as shown in Fig. 1A, and all rats were randomly divided into three groups. Rats in the normal group were untreated. Rats in the model group and Periplocin group were induced HFpEF as described in the method for 4 weeks and rats in the Periplocin group were given Periplocin (1.5 mg/kg) for additional 8 weeks (Fig. 1A). Marked abnormalities were observed in DOCA-salt rats, such as increased heart size, increased ratio of HW/BW, and increased concentration of NT-proBNP in the serum (Table 1, Fig. 1B–E), indicating a hypertensive cardiac remodeling. In addition, both systolic blood press (SBP) and diastolic blood pressure (DBP) were increased with a time-dependent manner during the 4 weeks of HFpEF modeling as reported [29] (Fig. 1F–G). Periplocin could significantly reduce the heart size, the ratios of HW/BW, and the concentration of serum NT-proBNP, but not the blood pressures (B–G), suggesting a protective effect of Periplocin against hypertensive cardiac remodeling.

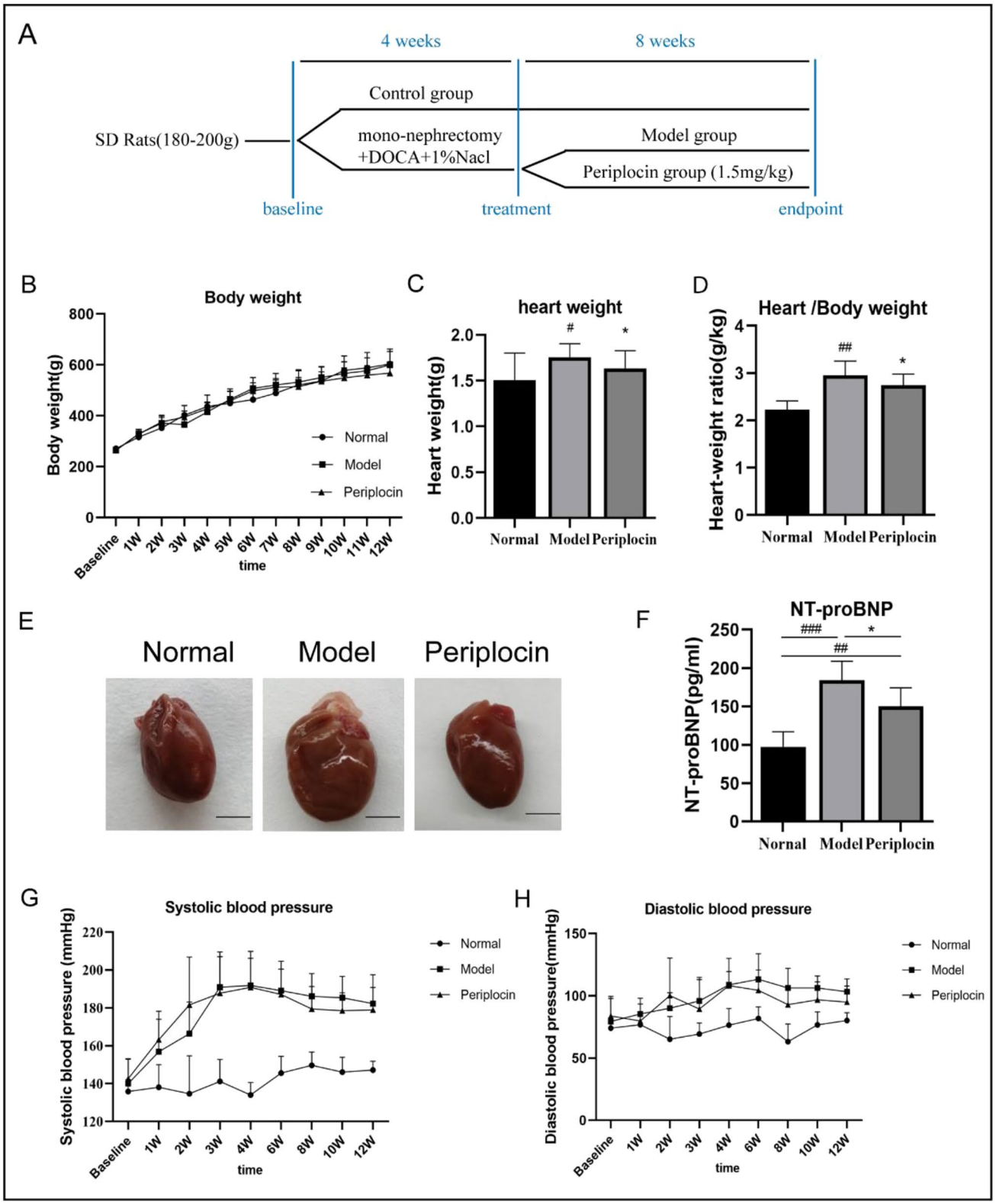

Fig. 1 Periplocin alleviated heart concentric remodeling in rats with HFpEF. **A** A schematic representative of study design. **B** Quantitative results of body weight, **C** heart weight, **D** and heart weight/body weight ratio in each group. **E** Representative images of hearts from rats of each group. **F** Serum NT-proBNP levels of the study groups. Both **G** systolic **H** and diastolic blood pressure in the model and Periplocin groups remained higher than in normal. #$p<0.05$, ##$p<0.01$, and ###$p<0.001$ versus normal group; *$p<0.05$, **$p<0.01$ versus model group, all by analysis of variance, $n=13$–15 in each group

Table 1 Basic parameters in each group at the 12 weeks of the experiment

	Normal	Model	Periplocin
Body weight (g)	518.01 ± 14.90	579.50 ± 53.46*	567.65 ± 43.75*
Heart weight (g)	1.25 ± 0.11	1.76 ± 0.15#	1.56 ± 0.21#*
HW/BW (g/kg)	2.37 ± 0.19	2.96 ± 0.29##	2.74 ± 0.23*
NT-proBNP (pg/mL)	97.39 ± 19.55	183.93 ± 24.11###	149.97 ± 24.29##*

#$p < 0.05$ vs normal, ##$p < 0.01$ vs normal; ###$p < 0.001$ vs normal *$p < 0.05$ vs model, **$p < 0.01$vs model

Periplocin Alleviated Left Ventricular Diastolic Dysfunction in Rats with HFpEF

To explore the structural changes in the left heart of HFpEF, echocardiography was performed and vital parameters were recorded (Table 2). Representative results from Typical M-mode and Doppler imaging are shown in Fig. 2A. Consistent with the cardiac structure characteristics of HFpEF, stroke volume, left ventricular volume, and E/A ratio were significantly decreased, while LVAW, LVPW, and IVRT were significantly increased in the model group compared to the normal group (Fig. 2B–G). Interestingly, 8 weeks Periplocin treatment resulted a significant rebound of cardiac structural remodeling parameters suggesting that Periplocin could effectively alleviate concentric LV remodeling in rats with HFpEF (Fig. 2B–G).

Table 2 Echocardiography parameters in each group at the 12 weeks of the experiment

	Normal	Model	Periplocin
Heart rate (BPM)	363.44 ± 31.33	353.95 ± 33.59	363.65 ± 29.29
IVRT (ms)	18.17 ± 3.69	20.80 ± 2.87#	18.28 ± 2.56*
IVCT (ms)	18.39 ± 6.31	18.49 ± 3.84	19.05 ± 4.35
E/A	1.15 ± 0.22	1.02 ± 0.26#	1.10 ± 0.17*
Volume; s (μL)	157.59 ± 76.90	222.26 ± 46.06#	179.98 ± 49.68
Volume; d (μL)	628.96 ± 182.65	575.94 ± 71.30#	671.82 ± 151.46
S.V. (μL)	519.94 ± 202.68	419.06 ± 111.09#	491.84 ± 125.35*
E.F. (%)	74.94 ± 6.22	67.44 ± 7.57#	72.88 ± 6.14
F.S. (%)	50.50 ± 13.43	44.89 ± 3.48	44.82 ± 5.97
LVAW (mm)	1.95 ± 0.38	2.31 ± 0.33#	2.09 ± 0.28*
LVPW (mm)	3.19 ± 0.45	3.81 ± 0.50#	3.37 ± 0.28*

#$p < 0.05$ vs control; ##$p < 0.01$ vs control; *$p < 0.05$ vs model; **$p < 0.01$ vs model

IVRT, isovolumic relaxation time; *IVCT*, isovolumic contraction time; *E*, passive peak left ventricular filling velocity; *A*, peak atrial systolic flow velocity; *S.V.*, stroke volume; *E.F.*, ejection fraction; *F.S.*, fractional shortening; *LVAW*, left ventricular anterior wall; *LVPW*, left ventricular posterior wall

To further evaluate the left ventricular diastolic function, we measured the commonly used parameters, including LVP, EDP, Diastolic Duration, ± dP/dt Max, and the left ventricular diastolic time constant (Tau) by invasive left heart catheter [30] (Table 3 and Fig. 2H–N). A significant reduced left ventricular compliance, impaired relaxation, and increased left ventricular filling pressures were found in the model group compared to the normal group, register as the increasing LVP, EDP, Diastolic Duration, and -dP/dt Max parameter (Fig. 2I–N). In addition, the Tau was markedly prolonged in the model group. As expected, the abnormal changes of left ventricular were significantly alleviated upon Periplocin treatment. However, the LVP remained high in the Periplocin group, indicating that Periplocin did not have a significant hypotensive effect (Fig. 2N). Representative record of the pressure–volume loop series at the endpoints is shown in Fig. 2H. The slope of the end-diastolic pressure–volume relationship was steeper in the model group compared with the other groups. Normalization of -dP/dt Max and Diastolic Duration in the Periplocin group confirmed that the increase in E/A ratio over time was due to normalization of left ventricular diastolic function. Of note, we did not observe any significant differences in heart rate and + dP/dt Max between the Periplocin and model groups.

Periplocin Prevented LV Fibrosis and Reduced Cardiac Inflammation

Furthermore, to investigate the effect of periplocin on LV fibrosis and cardiomyocyte hypertrophy in HFpEF, we subjected the heart paraffin samples for Masson trichrome staining and immunofluorescence staining with WGA and α-SMA antibodies. Strikingly, Periplocin treatment significantly alleviated the abnormal increased CSA area shown in the model of HFpEF (Fig. 3A, B). Additionally, LV fibrosis, collagen fiber proliferation, and inflammatory cell infiltration phenotypes in the model group, indicated by Masson trichrome staining and H&E staining, were significantly ameliorated upon Periplocin treatment in the Periplocin group (Fig. 3C, D). Concomitantly, Western blot and relative quantification results showed that the increased protein levels of MMP9, TGF-β, and NF-κB in the left ventricle of rats from the model group were reduced by Periplocin treatment

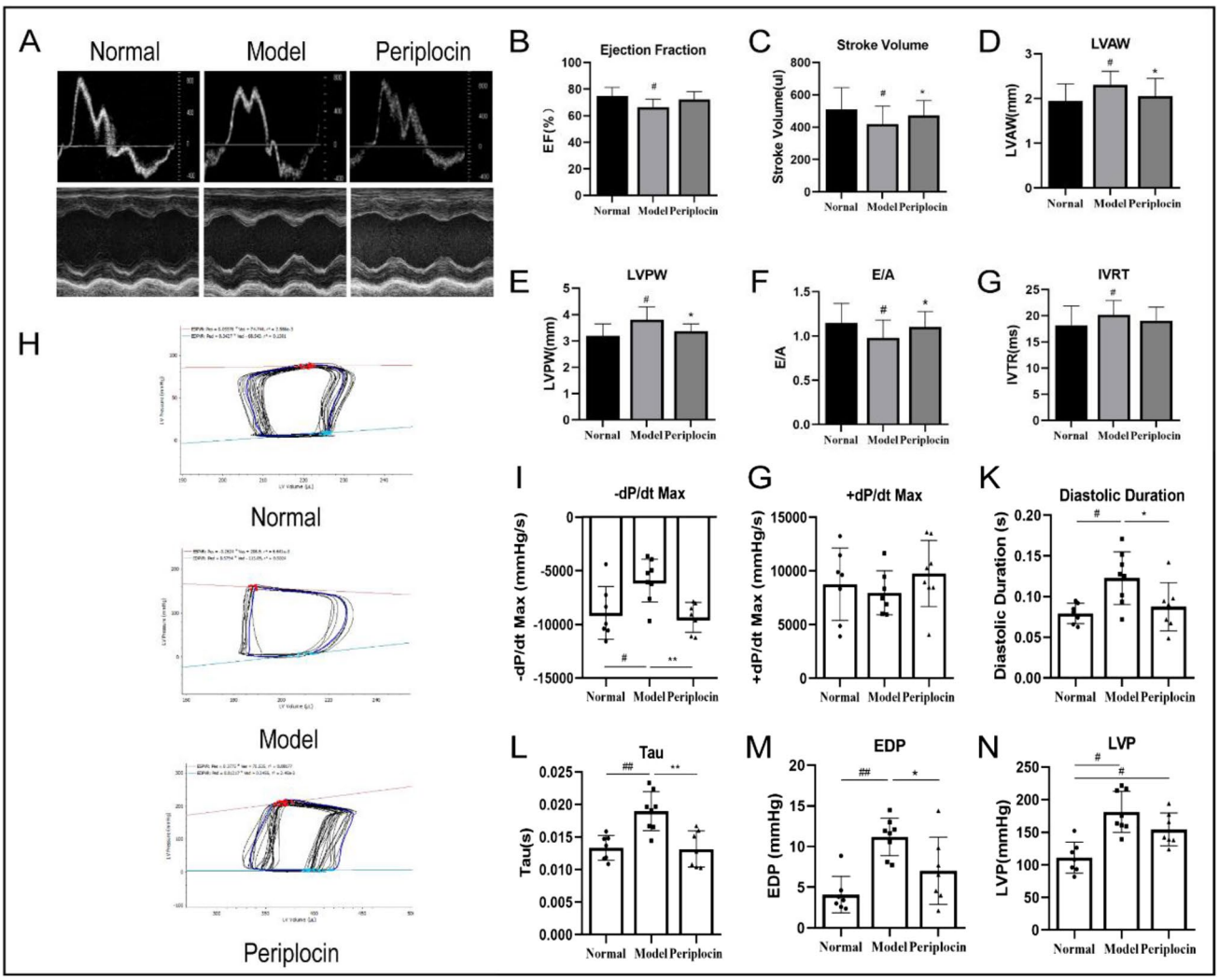

Fig. 2 Periplocin alleviated left ventricular diastolic dysfunction by echocardiography and hemodynamic analysis. **A** Representative images of transmittal flow by Doppler echocardiography (upper) and M-mode (lower) in each group. **B**–**E** Measurement in M-mode of left ventricular ejection fraction (**E**, **F**), stroke volume, left ventricular anterior wall (LVAW), left ventricular posterior wall (LVPW). **F**, **G** Measurement in Doppler echocardiography of E/A ratio and Isovolumic relaxation time (IVRT) ($n = 13$–15). **H** Representative pressure–volume (PV) loop recordings. Periplocin normalize **I** -dP/dt Max but with no change in **G** + dP/dt Max. **L** Tau, **M** Diastolic duration, and **M** left ventricular end-diastolic pressure (EDP) were also normalized after Periplocin-treated. However, **N** left ventricular pressure (LVP) is no significant difference between model and Periplocin animals ($n = 7$–8). $^{\#}p < 0.05$, $^{\#\#}p < 0.01$ versus normal; $^{*}p < 0.05$, $^{**}p < 0.05$ versus model group, all by analysis of variance

Table 3 Hemodynamic parameters in each group at the end of 12 weeks of the experiment

	Normal	Model	Periplocin
LVP (mmHg)	110.98 ± 23.82	181.30 ± 31.49#	194.30 ± 25.21
EDP (mmHg)	4.10 ± 2.23	11.2 ± 2.31##	5.89 ± 2.55*
Diastolic duration (s)	0.08 ± 0.01	0.12 ± 0.03#	0.10 ± 0.02*
+ dP/dt Max (mmHg/s)	8749.71 ± 3369.79	7954 ± 2050.49	9749.69 ± 3073.52
-dP/dt Max (mmHg/s)	− 8923.46 ± 2466.34	− 5917.29 ± 1985.81#	− 9333.98 ± 1386.63**
Tau (s)	0.0133 ± 0.0019	0.019 ± 0.003##	0.0132 ± 0.0028**

#$p < 0.05$ vs control; *$p < 0.05$ vs model; **$p < 0.01$ vs model

LVP, left ventricular pressure; *EDP*, end-diastolic pressure; ± *dP/dt Max*, maximal left ventricular pressure rising/dropping rate

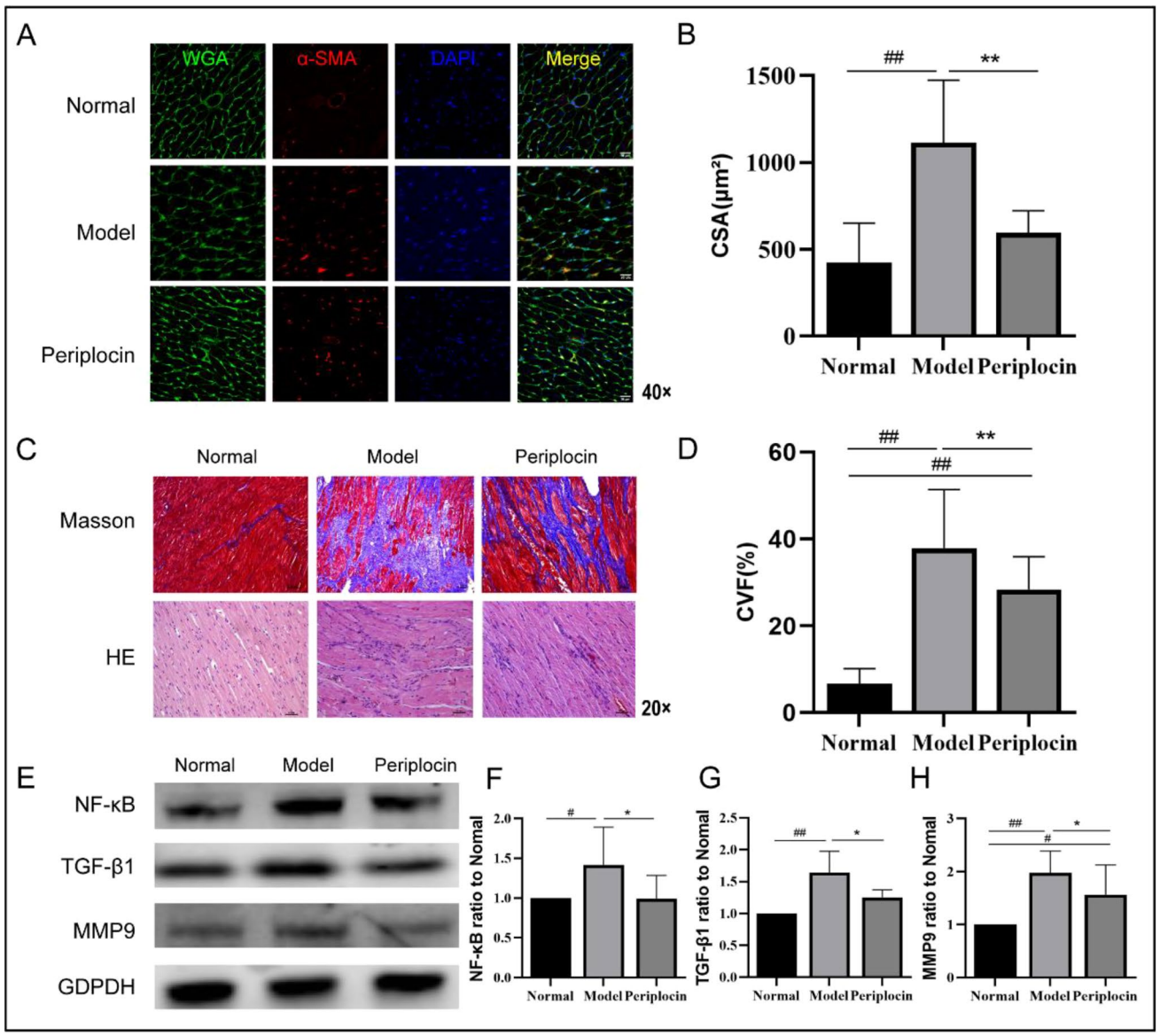

Fig. 3 Periplocin reversed myocardial remodeling and has an antifibrosis effect. **A**, **B** Representative images of wheat germ agglutinin (WGA) staining, and the calculated myocyte cross-sectional area (CSA). **C**, **D** Representative myocardial histological images of HE staining, Masson staining, and collagen volume fraction (CVF). **E**–**H** Matrix metallopeptidase 9 (MMP9), anti-nuclear factor kappa-B (NF-κB p65), anti-transforming growth factor beta 1 (TGF-β) content is higher in model than in normal and Periplocin rats, indicating significant fibrosis and myocarditis. #$p<0.05$, ##$p<0.01$, compared with the normal group; *$p<0.05$, **$p<0.01$, compared with the model group ($n=4$–6). All by analysis of variance

(Fig. 3E–H). We concluded that Periplocin prevented LV fibrosis and reduces cardiac inflammation.

Periplocin Enhanced the Cardiomyocyte Contractile Function and Intracellular Ca^{2+}. Transient Properties

To explore the effects of Periplocin on time parameters of cardiomyocyte contractile function and Ca^{2+} transient, we measured the related properties of ventricular myocytes isolated from rats. Treatment with Periplocin, a classical positive inotropic drug cardiac glycoside, increased sarcomere shortening and Ca^{2+} transient in a concentration-dependent manner, and the Sarc-L waveforms mirrored the Ca-ratio waveforms (Fig. 4A–D). Higher concentration of Periplocin resulted in longer Sarc-L times and calcium transient amplitudes. At the highest concentration of Periplocin (30 μM), the Sarc-L was increased to 254% ± 78.73%, and the calcium transient amplitude was increased to 138% ± 19.52% ($p<0.001$) (Fig. 4E, F).

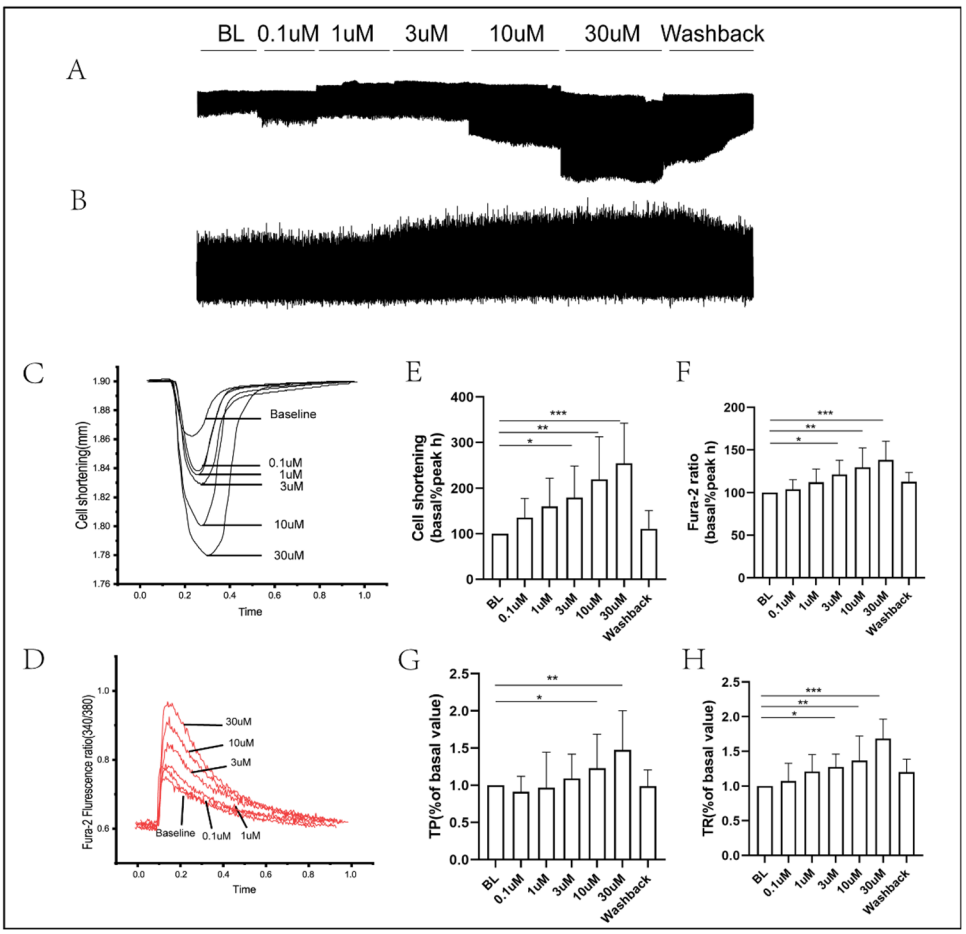

Fig. 4 Sarcomere shortening and Fura-2 $Ca.^{2+}$ transients from myocytes. **A**, **B** Representative myocyte traces of cell shortening (upper, Sarc-L) and Fura-2 ratio (lower, Ca-Ratio). **C**–**F** Average traces of cell shortening and Fura-2 ratio from the same myocyte at baseline, washout, and at each testing concentration of Periplocin. **G**, **H** Summary results of the time to 10% of the peak (TP) and the time to10% of the baseline (TR) for cell shortening before and after application of Periplocin. $*p<0.05$ vs BL, $**p<0.01$ vs BL, $***p<0.001$ vs BL ($n=10$). All by analysis of variance

To further evaluate the speed of cell contraction and cellular relaxation, we quantified Tp and the Tr, respectively (Fig. 4G, H). Compared with Baseline, Periplocin markedly increased the Tp to 122.96% ± 41.96% and 147% ± 48.28% (10 μM $p<0.05$, 30 μM $p<0.01$). Meanwhile, Tr was significantly increased to 127.56% ± 18.68%, 137.00% ± 27.55, and 168.38% ± 19.02% (3 μM $p<0.05$, 10 μM $p<0.01$, 30 μM $p<0.001$) after Periplocin treatment at relative concentration.

Taken together, the cardiomyocyte contractile and calcium transient data supported that Periplocin had a positive effect on cytosolic Ca^{2+}re-uptake, which resulted in more rapid myocyte contraction (shortening) and relaxation (relengthening) velocities.

Periplocin Inhibited Inflammation by Suppressing Immunocyte Recruitment in Rats with HFpEF

HFpEF is associated with increased circulating cytokines and infiltration of macrophages and other inflammatory cells in the heart [31]. To explore whether Periplocin has a role in reducing cardiac inflammation and initiating an immune response to alleviate HFpEF symptoms, flow cytometry analysis was employed to assess T cells, monocytes, and macrophages in the myocardium. We found that both $CD3^+CD4^+$ and $CD3^+CD8^+$ T-lymphocytes were significantly increased in the spleen and blood samples from the model group. Furthermore, a significant upregulated expression of inflammatory cytokines IFN-γ and IL-4 was observed, revealing a possible inflammatory recruitment of Th1 and Th2 subtypes in the model group. Upon 8 weeks treatment with Periplocin, the pro-inflammatory factor IFN-γ was significantly decreased, while the anti-inflammatory factor IL-4 was increased (Fig. 5A, B). Focusing on Treg cell populations, as a specific marker, $CD4^+CD25^+Foxp3^+$ cell population was significantly increased in the Periplocin group indicating that Periplocin treatment increased Treg cells and suppressed organismal inflammation (Fig. 5C, D). Due to the lack of commercially available rat antibodies, we focused on $CD11b/c^+$ isoforms to approximate the number of macrophages/monocytes in Fig. 5E, F. The percentage of $CD11b/c^+$ positive cells was increased in the model group and decreased in the Periplocin group compared to the model group individually. These results suggest that Periplocin might play a role as an immunomodulatory agent.

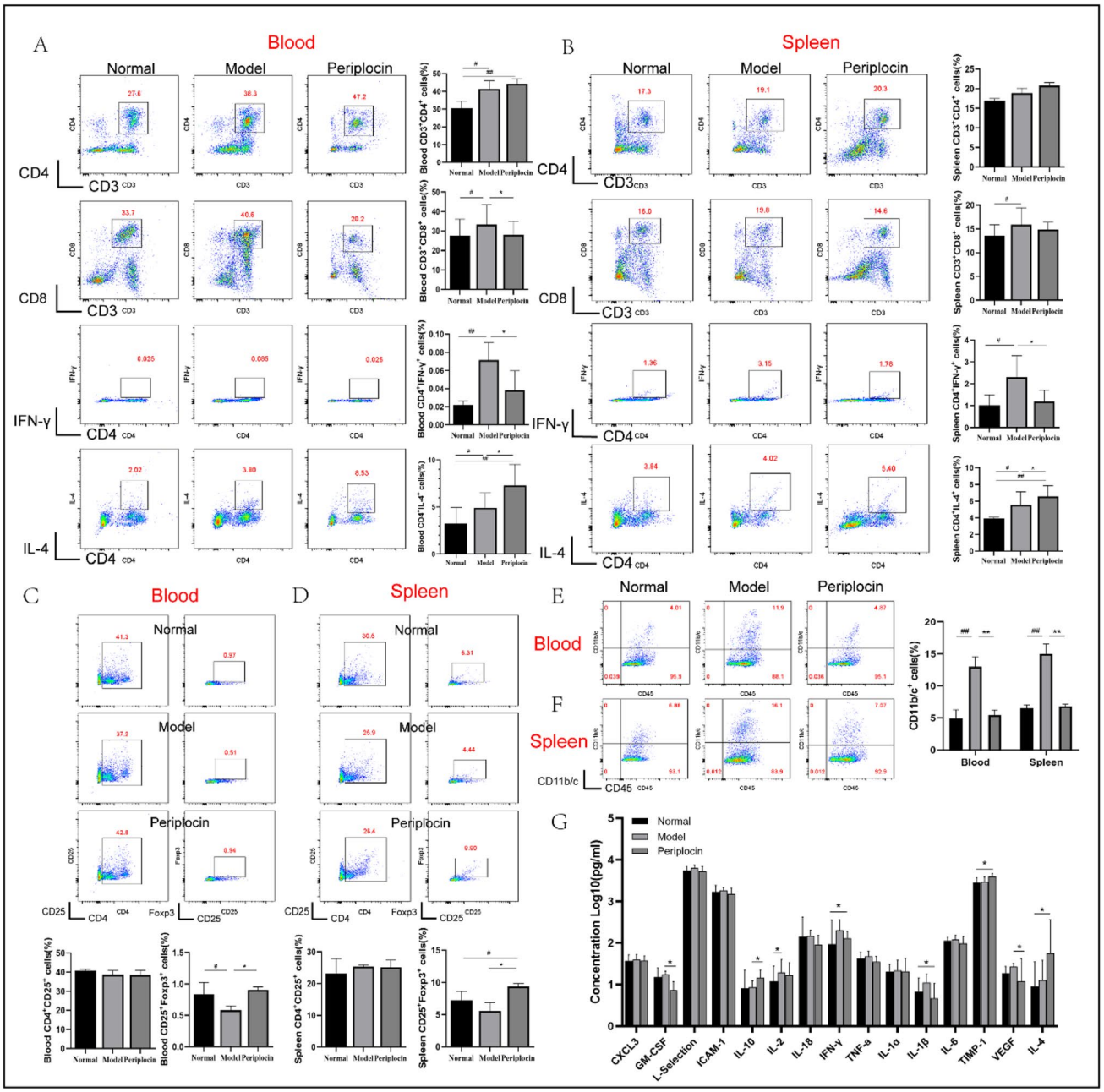

Fig. 5 Periplocin inhibits inflammation and immunocyte recruitment in HFpEF rats. **A**, **B** Representative lineage 1 (defined in the text) mononuclear cells and quantification within PBMC and spleen indicating that Periplocin can reduce the production of inflammatory cells and promote the secretion of anti-inflammatory cells. **C**, **D** Representative lineage 2 suggesting an increased number of Treg cells both in blood and spleen. **E**, **F** Representative lineage 3 of CD11b/c.$^{+}$ monocytes for macrophage/monocyte subpopulation identification. **G** Periplocin treatment normalizes the expression of pro-inflammatory cytokines in serum, including GM-CSF, IFN-γ, and IL-1β, and increases anti-inflammatory factors such as IL-10, IL-4, and TIMP-1. #$p < 0.05$, ##$p < 0.01$, compared with the normal group, *$p < 0.05$, **$p < 0.01$, compared with the model group. All by analysis of variance

To analyze the cytokine levels in serum, we turned to the Luminex assay multifactor assay. We found that Periplocin treatment decreased the expression of inflammatory cytokines such as GM-CSF, IFN-γ, IL-1β, and VEGF (Fig. 5G). On the other hand, the levels of anti-inflammatory cytokines such as IL-10, IL-4, and TIMP were increased in the Periplocin group. In summary, our findings demonstrate that Periplocin works as an immunomodulator in rat HFpEF models by inhibiting inflammatory response and suppressing the immunocyte recruitment.

Discussion

In the present study, we examined the protective effects of Periplocin, a kind of cardiac glycoside, on cardiac structure and function in a rat HFpEF model and clarified a potential anti-inflammatory function of Periplocin. After 8 weeks of treatment, Periplocin could significantly attenuate cardiac structural remodeling and improve cardiac function by improving the left ventricular ejection fraction and diastolic function, inhibiting cardiac hypotrophy, and decreasing the serum level of NT-ProBNP. Moreover, Periplocin could significantly inhibit inflammatory responses and immune cell recruitment in the hypertensive HFpEF rat model.

DOCA-salt rat model simulates most of the clinical manifestations caused by volume overload in humans, including hypertension, hypertrophy, fibrosis, electrical conduction abnormality, and vascular dysfunction, but does not affect the EF [29], which has been considered to be an angiotensin-independent animal model of HFpEF with the pathogenesis of oxidative stress, inflammatory reactions, and neurohumoral parasecretion [32]. Hypertension increases ventricular wall stress, which can be further exacerbated by chamber dilatation. To mitigate the increase in wall stress, the wall thickness (i.e., hypertrophy) will be increased so that to allow more sarcomere units share the workload [33]. Cardiac hypertrophy, an indicator of ventricular remodeling, was clinically manifested as HFpEF and an important determinant of patient morbidity and long-term outcomes [34]. In this study, we reported that the ventricular remodeling indexes, including the cardiac index, NT-ProBNP, LVAW, and LVPW, were markedly reduced in the Periplocin group compared to those in the model group. Moreover, the WGA staining results demonstrated that the cross-sectional area of cardiomyocytes in the Periplocin group was decreased. Consistently, both the echocardiography test results and the WGA staining results indicated the effect of Periplocin on attenuating cardiomyocyte hypertrophy.

An impairment of relaxation is readily detected by a prolongation of IVRT, diastolic duration, Tau time, and the ratio between early and late filling (E/A ratio)[35]. In this study, the DOCA-salt rats manifested the typical diastolic dysfunctions characterized by delayed early relaxation, myocardial and myocyte stiffening, and associated changes in hemodynamic [36–38]. The attenuation in diastolic function upon Periplocin treatment was not only limited to the early active phase of diastole, which registered as the shortening of the isovolumic relaxation constant (Tau) and the reduction in the minimum rate of ventricular pressure change (dP/dt min), but also existed in the late passive phase of diastole such as the end-diastolic pressure–volume relationship (EDPVR slope).

Changes in collagen and titin homeostasis are the main contributors to the increase in passive myocardial stiffness, which is a major component of diastolic impairment in HFpEF [39]. In DOCA-salt rats, hypertension induces leukocyte extravasation in heart tissue, which may further result in increasing collagen deposition and ventricular stiffness [40]. MMPs, who promote the turnover of the extracellular matrix, have been suggested as biomarkers for the diagnosis and prognosis of HFpEF [41]. In this study, Periplocin significantly decreased the cardiac fibrosis and the myofibroblast infiltration in the Periplocin group compared with the model group. Consistently, the expression of MMP9, a fibrosis indicator, was also decreased. All the data suggested that Periplocin played an effective role in improving left ventricular diastolic function by reducing ventricular stiffness and increasing left ventricular compliance.

Fibrogenesis is due to excesses of the same biologic events involved in normal tissue repair. Tissue repair is usually associated with an inflammatory response [42]. Persistent inflammation has a pivot role in the pathogenesis of chronic heart failure. The upregulation of inflammatory mediators and pro-inflammatory cytokines leads to the activation of fibroblasts and the infiltration of immune-inflammatory cells, which initiate ventricular remodeling [40]. Experimental studies reported an increase in inflammatory response in patients with HFpEF [8]. Since the immune system disorder mediated by systemic inflammation plays an essential role in the pathogenesis of HFpEF, we predicted that the additional benefits of Periplocin therapy might be associated with further inhibition of inflammation. In this study, systemic T cell activation and infiltration of T cells, monocytes, and macrophages were observed in spleen/blood samples from rats with HFpEF. T cells are present in non-ischemic heart failure and dominate the immune response [43]. Here, we designed an experiment to evaluate the subpopulations of T cells in our rat model. We found that $CD8^+$ T cells, $CD4^+$ T cells, and Th1 cells were significantly enriched and while their cytokine, IFN-γ, was upregulated, suggesting an obvious pro-inflammatory response in rats with HFpEF. Periplocin treatment could significantly reduce HFpEF-induced enrichment of immune cells and significantly upregulate the expression of Th2 polarized cytokine, IL-4. Additionally, there is a Th17/Treg cell imbalance in HFpEF patients [44]. Treg cell reduction exacerbates myocardial fibrosis and heart failure, while upregulation of Treg improves cardiac insufficiency in patients with chronic heart failure [45]. Interestingly, Periplocin treatment increased Treg cells and suppressed cardiac inflammation in rats with HFpEF. Moreover, Periplocin significantly reduced the invasion of $CD11b/c^+$ monocytes/macrophages, which play a role in hypertrophic cardiomyocytes [46]. Meanwhile, studies have shown that Periplocin could decrease the expression of cytokines, including TNF-α, IL-1β, IL-6,

and proteins, including p-IκBα/IκBα and pNF-κB/NF-κB, in rheumatoid arthritis [20]. TGF-β induces inflammation by producing cytokines and chemokines, and stimulating the recruitment and activation of inflammatory cells [47]. Our data confirmed that Periplocin decreased the expression of TGF-β and NF-κB in HFpEF rats, which subsequently inhibited the collagen production and inflammatory recruitment. Furthermore, Periplocin downregulated pro-inflammatory cytokines, including GM-CSF, IFN-γ, IL-1β, and VEGF, and upregulated anti-inflammatory cytokines, including IL-10 and IL-4, in blood samples collected from DOCA rats. Thus, we proved that Periplocin played an anti-inflammatory role by decreasing inflammatory cytokines, preventing myocardial inflammation, and inhibiting inflammatory responses and immune cell recruitment in HFpEF rats, which might also contribute to the effective function of Periplocin in improving cardiac function and ventricular remodeling.

Researchers have shown that diastolic dysfunction may be due to the partial inactivation of ion channels, which will lead to increase of intracellular diastolic Ca^{2+} concentrations [48]. Digitalis cardiac glycosides are characterized by enhancing cardiac contractility in heart failure, and facilitating Ca^{2+} uptake through Na^{+}/Ca^{2+} exchange [49]. Since regulation of calcium homeostasis is essential for maintaining normal cardiac diastolic and systolic function [50], our study demonstrated that Periplocin could enhance myocardial cell contractility and increase on cell shortening and calcium transient in a dose-dependent manner. Furthermore, we found that Periplocin increased both Tp and Tr, which are essential parameters for the speed of cell contraction and cellular relaxation, indicating a positive effect of Periplocin on increasing the systolic and diastolic functions of cardiomyocytes simultaneously.

Although we demonstrated that Periplocin had a great potential in the treatment of HFpEF, there were still several limitations. It was elusive how Periplocin directed the proliferation or differentiation of cardiac macrophages in the rat HFpEF model. Moreover, it was also unclear whether long-term periplocin could still improve HFpEF cardiac function.

Conclusion

Undoubtedly, there is a great unmet need to develop new therapeutic options for the treatment of HFpEF. We found that Periplocin improved cardiac function, normalized LV relaxation, ameliorated diastolic dysfunction, prevented left ventricular hypertrophy, and reduced myocardial fibrosis in HFpEF rats. Given that the tolerance and safety of cardiac glycosides are clinically acceptable [51], results from our data suggested it is worth repurposing Periplocin as a new therapeutic option for HFpEF.

Acknowledgements We acknowledge the valuable help in grammar and syntax corrections on this manuscript performed by Dr. Hui Qi.

Funding This study was supported by the National Key Research and Development Program (grant NO. 2017YFC1700500), the Natural Science Foundation of Hebei Province (H2019106059), and the Scientific Research Plan Project of Hebei Administration of Traditional Chinese Medicine (No. Z2022020).

Declarations

Ethics Approval All animals were handled and maintained under the Animal Care and Use Committee of Hebei Yiling Chinese Medicine Research Institute (NO. 2021024). No human studies were carried out by the authors for this article.

Conflict of Interest The authors declare no competing interests.

References

1. Upadhya, B., & Kitzman, D. W. (2020). Heart failure with preserved ejection fraction: New approaches to diagnosis and management. *Clinical Cardiology, 43*(2), 145–155. https://doi.org/10.1002/clc.23321
2. Shear, F. E. (2019). Novel paradigms in the therapeutic management of heart failure with preserved ejection fraction: Clinical perspectives. *American Journal of Cardiovascular Diseases, 9*(5), 91–108.
3. Shah, K. S., Xu, H., Matsouaka, R. A., Bhatt, D. L., Heidenreich, P. A., Hernandez, A. F., Devore, A. D., Yancy, C. W., & Fonarow, G. C. (2017). Heart failure with preserved, borderline, and reduced ejection fraction: 5-year outcomes. *Journal of the American College of Cardiology, 70*(20), 2476–2486. https://doi.org/10.1016/j.jacc.2017.08.074
4. Minamisawa, M., Claggett, B., Suzuki, K., Hegde, S. M., Shah, A. M., Desai, A. S., Lewis, E. F., Shah, S. J., Sweitzer, N. K., Fang, J. C., Anand, I. S., O'Meara, E., Rouleau, J. L., Pitt, B., Pfeffer, M. A., Solomon, S. D., & Vardeny, O. (2021). Association of hyper-polypharmacy with clinical outcomes in heart failure with preserved ejection fraction. *Circulation. Heart Failure, 14*(11), e8293. https://doi.org/10.1161/CIRCHEARTFAILURE.120.008293
5. Simmonds, S. J., Cuijpers, I., Heymans, S., Jones, E. (2020). Cellular and molecular differences between HFpEF and HFrEF: A step ahead in an improved pathological understanding. Cells-Basel 9(1). https://doi.org/10.3390/cells9010242
6. Campanharo, F. F., Cecatti, J. G., Haddad, S. M., Parpinelli, M. A., Born, D., Costa, M. L., & Mattar, R. (2015). The impact of cardiac diseases during pregnancy on severe maternal morbidity and mortality in Brazil. *PLoS One, 10*(12), e144385. https://doi.org/10.1371/journal.pone.0144385
7. Rossi, A., Gheorghiade, M., Triposkiadis, F., Solomon, S. D., Pieske, B., & Butler, J. (2014). Left atrium in heart failure with preserved ejection fraction: Structure, function, and significance. *Circulation Heart Failure, 7*(6), 1042–1049. https://doi.org/10.1161/CIRCHEARTFAILURE.114.001276
8. van Empel, V., & Brunner-La, R. H. (2015). Inflammation in HFpEF: Key or circumstantial? *International Journal of Cardiology, 189*, 259–263. https://doi.org/10.1016/j.ijcard.2015.04.110
9. Singh, S., Moore, H., Karasik, P. E., Lam, P. H., Wopperer, S., Arundel, C., Tummala, L., Anker, M. S., Faselis, C., Deedwania, P., Morgan, C. J., Zeng, Q., Allman, R. M., Fonarow, G. C., &

Ahmed, A. (2020). Digoxin initiation and outcomes in patients with heart failure (HFrEF and HFpEF) and atrial fibrillation. *American Journal of Medicine, 133*(12), 1460–1470. https://doi.org/10.1016/j.amjmed.2020.05.030
10. Gheorghiade, M., & Ferguson, D. (1991). Digoxin. A neurohormonal modulator in heart failure? *Circulation, 84*(5), 2181–2186. https://doi.org/10.1161/01.cir.84.5.2181
11. Ferguson, D. W., Berg, W. J., Sanders, J. S., Roach, P. J., Kempf, J. S., & Kienzle, M. G. (1989). Sympathoinhibitory responses to digitalis glycosides in heart failure patients. Direct evidence from sympathetic neural recordings. *Circulation, 80*(1), 65–77. https://doi.org/10.1161/01.cir.80.1.65
12. Vogel, R., Kirch, D., LeFree, M., Frischknecht, J., & Steele, P. (1977). Effects of digitalis on resting and isometric exercise myocardial perfusion in patients with coronary artery disease and left ventricular dysfunction. *Circulation, 56*(3), 355–359. https://doi.org/10.1161/01.cir.56.3.355
13. Firth, B. G., Dehmer, G. J., Corbett, J. R., Lewis, S. E., Parkey, R. W., & Willerson, J. T. (1980). Effect of chronic oral digoxin therapy on ventricular function at rest and peak exercise in patients with ischemic heart disease. *American Journal of Cardiology, 46*(3), 481–490. https://doi.org/10.1016/0002-9149(80)90019-3
14. Sonnenblick, E. H., Williams, J. J., Glick, G., Mason, D. T., & Braunwald, E. (1966). Studies on digitalis XV. Effects of cardiac glycosides on myocardial force-velocity relations in the nonfailing human heart. *Circulation, 34*(3), 532–539. https://doi.org/10.1161/01.cir.34.3.532
15. Adamantidis, M. M., Duriez, P. R., Vincent, A. C., & Dupuis, B. A. (1983). Digoxin-induced toxicity and experimental atrioventricular block in dogs. Relation between ventricular arrhythmias and oscillatory afterpotentials. *Journal of Pharmacology, 14*(3), 333–349.
16. Capasso, J. M., Puntillo, E., Halpryn, B., Olivetti, G., Li, P., & Anversa, P. (1992). Amelioration of effects of hypertension and diabetes on myocardium by cardiac glycoside. *American Journal of Physiology, 262*(3 Pt 2), H734–H742. https://doi.org/10.1152/ajpheart.1992.262.3.H734
17. Zile, M. R., & Brutsaert, D. L. (2002). New concepts in diastolic dysfunction and diastolic heart failure: Part II: Causal mechanisms and treatment. *Circulation, 105*(12), 1503–1508. https://doi.org/10.1161/hc1202.105290
18. National Pharmacopoeia Committee. (2020). *Chinese Pharmacopoeia-Volume I* (pp. 1088–1089). Beijing: China Medical Science and Technology Press.
19. Xie, G., Sun, L., Li, Y., Chen, B., & Wang, C. (2021). Periplocin inhibits the growth of pancreatic cancer by inducing apoptosis via AMPK-mTOR signaling. *Cancer Medicine, 10*(1), 325–336. https://doi.org/10.1002/cam4.3611
20. Zhang, X., Nan, H., Guo, J., Yang, S., & Liu, J. (2020). Periplocin induces apoptosis and inhibits inflammation in rheumatoid arthritis fibroblast-like synoviocytes via nuclear factor kappa B pathway. *IUBMB Life, 72*(9), 1951–1959. https://doi.org/10.1002/iub.2328
21. Haohao, C., Xiaoming, W., Guixiang, P., & Tingting, L. (2017). Detection of the human plasma protein binding rate of periplocin, periplocymarin and periplogenin. *Journal of Liaoning University of TCM, 19*(07), 32–35. https://doi.org/10.13194/j.issn.1673-842x.2017.07.007
22. Zhang, W. J., Song, Z. B., Bao, Y. L., Li, W. L., Yang, X. G., Wang, Q., Yu, C. L., Sun, L. G., Huang, Y. X., & Li, Y. X. (2016). Periplogenin induces necroptotic cell death through oxidative stress in HaCaT cells and ameliorates skin lesions in the TPA- and IMQ-induced psoriasis-like mouse models. *Biochemical Pharmacology, 105*, 66–79. https://doi.org/10.1016/j.bcp.2016.02.001
23. Da, S., Jing, Z., Jin-tang, C., Kun, Z., & Yan-ru, D. (2011). Comparison of the effect of cardiac glycosides in periplocae cortex on isolated heart in rats. *Chinese Archives of Traditional Chinese Medicine, 29*(12), 2633–2635. https://doi.org/10.13193/j.archtcm.2011.12.35.sund.054
24. Li, M., Yan-su, J., Juan, H., Fang, L., & Yi, W. (2008). Effect of glucoperiplocymarin on left ventricular structure and function in chronic heart failure rats by color doppler- echocardiography. *Journal of Tianjin University of Traditional Chinese Medicine, 02*, 81–83.
25. Silberman, G. A., Fan, T. H., Liu, H., Jiao, Z., Xiao, H. D., Lovelock, J. D., Boulden, B. M., Widder, J., Fredd, S., Bernstein, K. E., Wolska, B. M., Dikalov, S., Harrison, D. G., & Dudley, S. J. (2010). Uncoupled cardiac nitric oxide synthase mediates diastolic dysfunction. *Circulation, 121*(4), 519–528. https://doi.org/10.1161/CIRCULATIONAHA.109.883777
26. Gao, Y., Zhang, K., Zhu, F., Wu, Z., Chu, X., Zhang, X., Zhang, Y., Zhang, J., & Chu, L. (2014). Salvia miltiorrhiza (Danshen) inhibits L-type calcium current and attenuates calcium transient and contractility in rat ventricular myocytes. *J Ethnopharmacol, 158 Pt A*, 397–403. https://doi.org/10.1016/j.jep.2014.10.049
27. Salem, K. A., Qureshi, A., Ljubisavijevic, M., Oz, M., Isaev, D., Hussain, M., & Howarth, F. C. (2010). Alloxan reduces amplitude of ventricular myocyte shortening and intracellular Ca2+ without altering L-type Ca2+ current, sarcoplasmic reticulum Ca2+ content or myofilament sensitivity to Ca2+ in Wistar rats. *Molecular and Cellular Biochemistry, 340*(1–2), 115–123. https://doi.org/10.1007/s11010-010-0408-7
28. Lavelle, G. C., Sturman, L., & Hadlow, W. J. (1972). Isolation from mouse spleen of cell populations with high specific infectivity for scrapie virus. *Infection and Immunity, 5*(3), 319–323. https://doi.org/10.1128/iai.5.3.319-323.1972
29. Iyer, A., Chan, V., & Brown, L. (2010). The DOCA-salt hypertensive rat as a model of cardiovascular oxidative and inflammatory stress. *Current Cardiology Reviews, 6*(4), 291–297. https://doi.org/10.2174/157340310793566109
30. Andersen, M. J., & Borlaug, B. A. (2014). Invasive hemodynamic characterization of heart failure with preserved ejection fraction. *Heart Failure Clinics, 10*(3), 435–444. https://doi.org/10.1016/j.hfc.2014.03.001
31. Glezeva, N., & Baugh, J. A. (2014). Role of inflammation in the pathogenesis of heart failure with preserved ejection fraction and its potential as a therapeutic target. *Heart Failure Reviews, 19*(5), 681–694. https://doi.org/10.1007/s10741-013-9405-8
32. Loch, D., Hoey, A., & Brown, L. (2006). Attenuation of cardiovascular remodeling in DOCA-salt rats by the vasopeptidase inhibitor, omapatrilat. *Clinical and Experimental Hypertension, 28*(5), 475–488. https://doi.org/10.1080/10641960600798754
33. Connelly, K. A., Zhang, Y., Visram, A., Advani, A., Batchu, S. N., Desjardins, J. F., Thai, K., & Gilbert, R. E. (2019). Empagliflozin improves diastolic function in a nondiabetic rodent model of heart failure with preserved ejection fraction. *JACC Basic Transl Sci, 4*(1), 27–37. https://doi.org/10.1016/j.jacbts.2018.11.010
34. Konstam, M. A., Kramer, D. G., Patel, A. R., Maron, M. S., & Udelson, J. E. (2011). Left ventricular remodeling in heart failure: Current concepts in clinical significance and assessment. *JACC: Cardiovascular Imaging, 4*(1), 98–108. https://doi.org/10.1016/j.jcmg.2010.10.008
35. Nagueh, S. F., Smiseth, O. A., Appleton, C. P., Byrd, B. R., Dokainish, H., Edvardsen, T., Flachskampf, F. A., Gillebert, T. C., Klein, A. L., Lancellotti, P., Marino, P., Oh, J. K., Popescu, B. A., & Waggoner, A. D. (2016). Recommendations for the evaluation of left ventricular diastolic function by echocardiography: An update from the American Society of Echocardiography and the European Association of Cardiovascular Imaging. *Journal of the American Society of Echocardiography, 29*(4), 277–314. https://doi.org/10.1016/j.echo.2016.01.011

36. Sharma, K., & Kass, D. A. (2014). Heart failure with preserved ejection fraction: Mechanisms, clinical features, and therapies. *Circulation Research, 115*(1), 79–96. https://doi.org/10.1161/CIRCRESAHA.115.302922
37. Kass, D. A. (2000). Assessment of diastolic dysfunction. Invasive modalities. *Cardiology Clinical, 18*(3), 571–586. https://doi.org/10.1016/s0733-8651(05)70162-4
38. Yellin, E. L., & Meisner, J. S. (2000). Physiology of diastolic function and transmitral pressure-flow relations. *Cardiology Clinics, 18*(3), 411–433. https://doi.org/10.1016/s0733-8651(05)70153-3
39. Zile, M. R., Baicu, C. F., Ikonomidis, J. S., Stroud, R. E., Nietert, P. J., Bradshaw, A. D., Slater, R., Palmer, B. M., Van Buren, P., Meyer, M., Redfield, M. M., Bull, D. A., Granzier, H. L., & LeWinter, M. M. (2015). Myocardial stiffness in patients with heart failure and a preserved ejection fraction: Contributions of collagen and titin. *Circulation, 131*(14), 1247–1259. https://doi.org/10.1161/CIRCULATIONAHA.114.013215
40. Iyer, A., Woodruff, T. M., Wu, M. C., Stylianou, C., Reid, R. C., Fairlie, D. P., Taylor, S. M., & Brown, L. (2011). Inhibition of inflammation and fibrosis by a complement C5a receptor antagonist in DOCA-salt hypertensive rats. *Journal of Cardiovascular Pharmacology, 58*(5), 479–486. https://doi.org/10.1097/FJC.0b013e31822a7a09
41. Zouein, F. A., de Castro, B. L., Da, C. D., Lindsey, M. L., Kurdi, M., & Booz, G. W. (2013). Heart failure with preserved ejection fraction: Emerging drug strategies. *Journal of Cardiovascular Pharmacology, 62*(1), 13–21. https://doi.org/10.1097/FJC.0b013e31829a4e61
42. Nicoletti, A., Heudes, D., Mandet, C., Hinglais, N., Bariety, J., & Michel, J. B. (1996). Inflammatory cells and myocardial fibrosis: Spatial and temporal distribution in renovascular hypertensive rats. *Cardiovascular Research, 32*(6), 1096–1107. https://doi.org/10.1016/s0008-6363(96)00158-7
43. Nevers, T., Salvador, A. M., Grodecki-Pena, A., Knapp, A., Velazquez, F., Aronovitz, M., Kapur, N. K., Karas, R. H., Blanton, R. M., & Alcaide, P. (2015). Left ventricular T-cell recruitment contributes to the pathogenesis of heart failure. *Circulation. Heart Failure, 8*(4), 776–787. https://doi.org/10.1161/CIRCHEARTFAILURE.115.002225
44. Li, N., Bian, H., Zhang, J., Li, X., Ji, X., & Zhang, Y. (2010). The Th17/Treg imbalance exists in patients with heart failure with normal ejection fraction and heart failure with reduced ejection fraction. *Clinica Chimica Acta, 411*(23–24), 1963–1968. https://doi.org/10.1016/j.cca.2010.08.013
45. Lu, M., Qin, X., Yao, J., Yang, Y., Zhao, M., & Sun, L. (2020). Th17/Treg imbalance modulates rat myocardial fibrosis and heart failure by regulating LOX expression. *Acta Psychologica, 230*(3), e13537. https://doi.org/10.1111/apha.13537
46. Keck, M., Flamant, M., Mougenot, N., Favier, S., Atassi, F., Barbier, C., Nadaud, S., Lompre, A. M., Hulot, J. S., & Pavoine, C. (2019). Cardiac inflammatory CD11b/c cells exert a protective role in hypertrophied cardiomyocyte by promoting TNFR2- and Orai3- dependent signaling. *Science and Reports, 9*(1), 6047. https://doi.org/10.1038/s41598-019-42452-y
47. Cao, H., Xiao, C., He, Z., Huang, H., & Tang, H. (2021). IgE and TGF-beta signaling: From immune to cardiac remodeling. *Journal of Inflammation Research, 14*, 5523–5526. https://doi.org/10.2147/JIR.S332591
48. Lovelock, J. D., Monasky, M. M., Jeong, E. M., Lardin, H. A., Liu, H., Patel, B. G., Taglieri, D. M., Gu, L., Kumar, P., Pokhrel, N., Zeng, D., Belardinelli, L., Sorescu, D., Solaro, R. J., & Dudley, S. J. (2012). Ranolazine improves cardiac diastolic dysfunction through modulation of myofilament calcium sensitivity. *Circulation Research, 110*(6), 841–850. https://doi.org/10.1161/CIRCRESAHA.111.258251
49. Blaustein, M. P., Juhaszova, M., & Golovina, V. A. (1998). The cellular mechanism of action of cardiotonic steroids: A new hypothesis. *Clinical and Experimental Hypertension, 20*(5–6), 691–703. https://doi.org/10.3109/10641969809053247
50. Barry, W. H., & Bridge, J. H. (1993). Intracellular calcium homeostasis in cardiac myocytes. *Circulation, 87*(6), 1806–1815. https://doi.org/10.1161/01.cir.87.6.1806
51. Zhao, R., Han, C., Dai, S., Wei, S., Xiang, X., Wang, Y., Zhao, R., Zhao, L., & Shan, B. (2021). Inhibitory effects of periplocin on lymphoma cells: A network pharmacology approach and experimental validation. *Drug Des Devel Ther, 15*, 1333–1344. https://doi.org/10.2147/DDDT.S302221